# What can we learn from strong lensing ?


## Frédéric Courbin (EPFL, Switzerland)


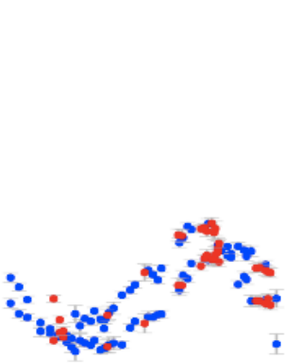

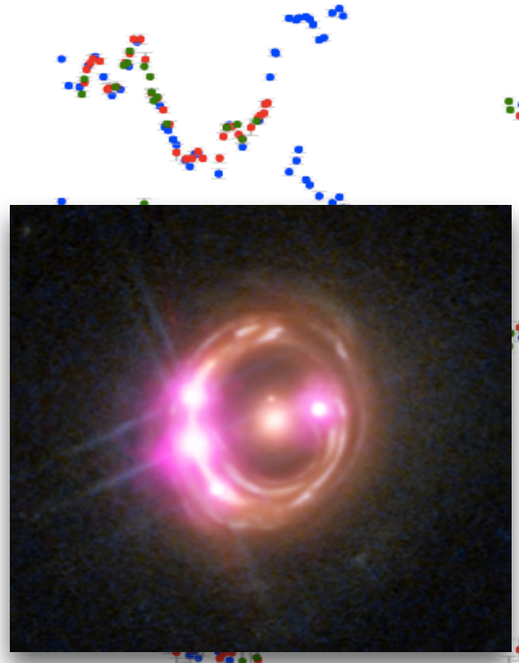

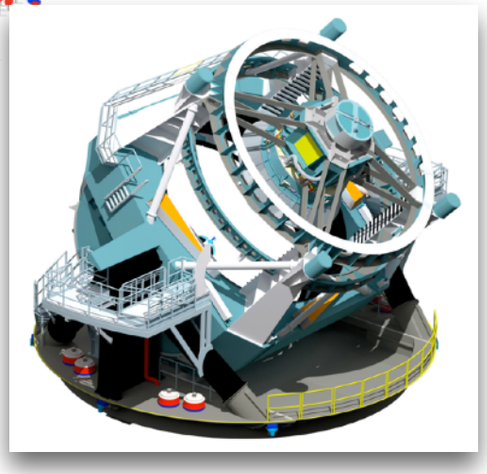


EPFL Laboratoire d'astrophysique http://lastro.epfl.ch
Ecole Polytechnique Fédérale de Lausanne (EPFL)


Lausanne - February 2020

# Observables

- Deflection angles (total masses in apertures)
- Magnification (gravitational telescope and microscope)
- Time delay (cosmography)
- Ratio of distances (cosmography)

**BUT**

- Degeneracies in lens models (mass-slope and mass-sheet)
- Contribution from the whole line of sight up to the source redshift
- Small sample sizes + no homogeneous samples (so far)
- Source structure effects

# Example of RX J1131-123

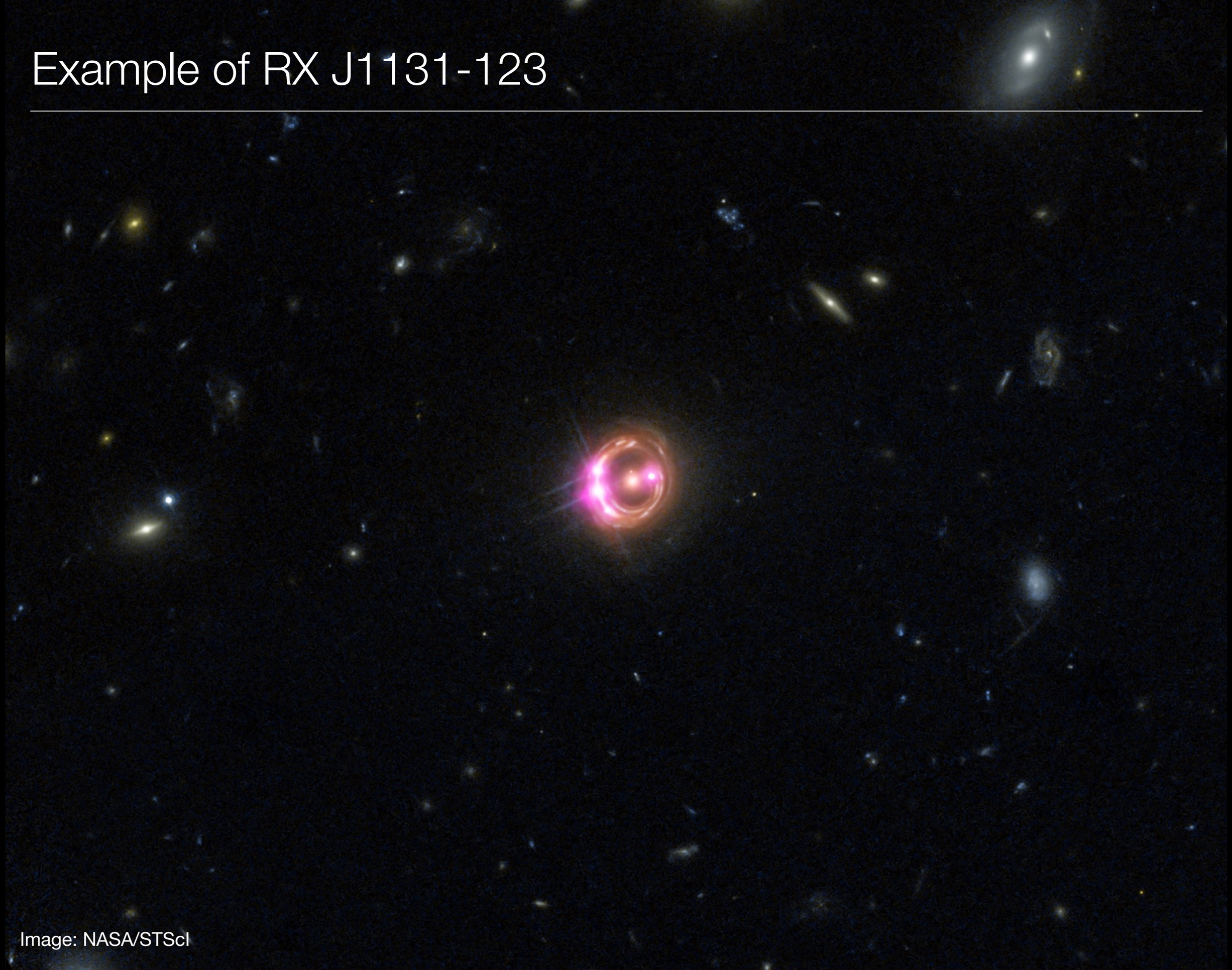

Image: NASA/STScI

# Example of RX J1131-123

Mass in the Einstein ring
Mass slope at image position

Image: NASA/STScI

# Example of RX J1131-123

Mass in the Einstein ring
Mass slope at image position

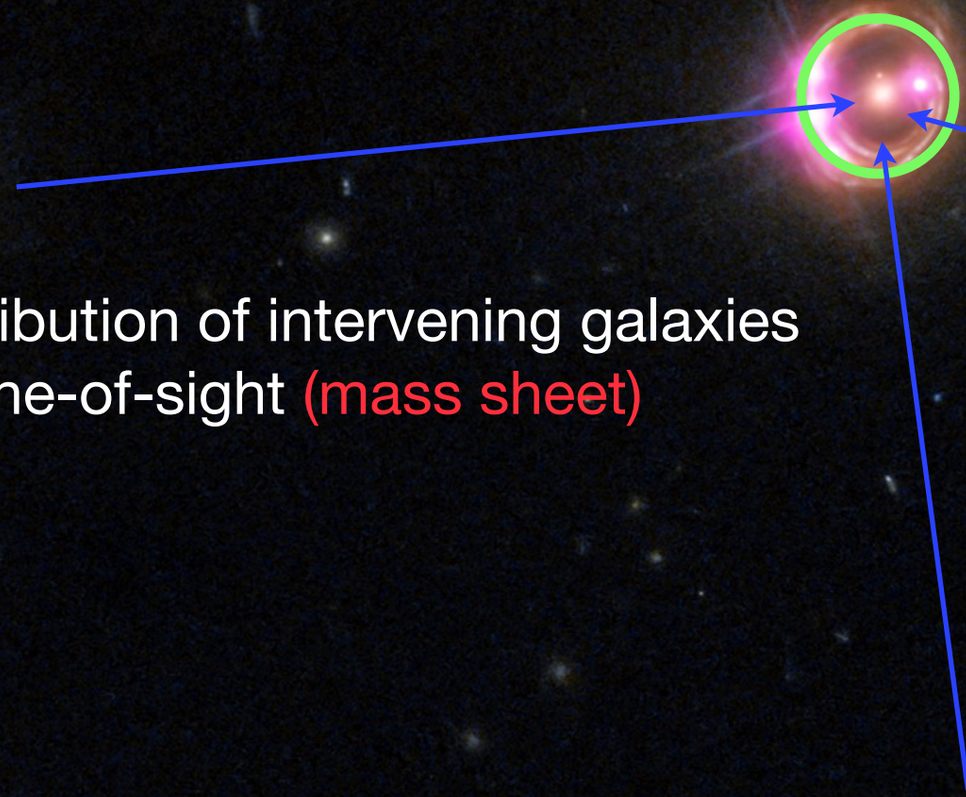

Mass contribution of intervening galaxies
along the line-of-sight (mass sheet)

Image: NASA/STScI

# Example of RX J1131-123

Substructures in the main lens modify
- image positions
- image shape
- image magnification
- time delays

Image: NASA/STScI

# Example of RX J1131-123

Substructures in the main lens modify
- image positions
- image shape
- image magnification
- time delays

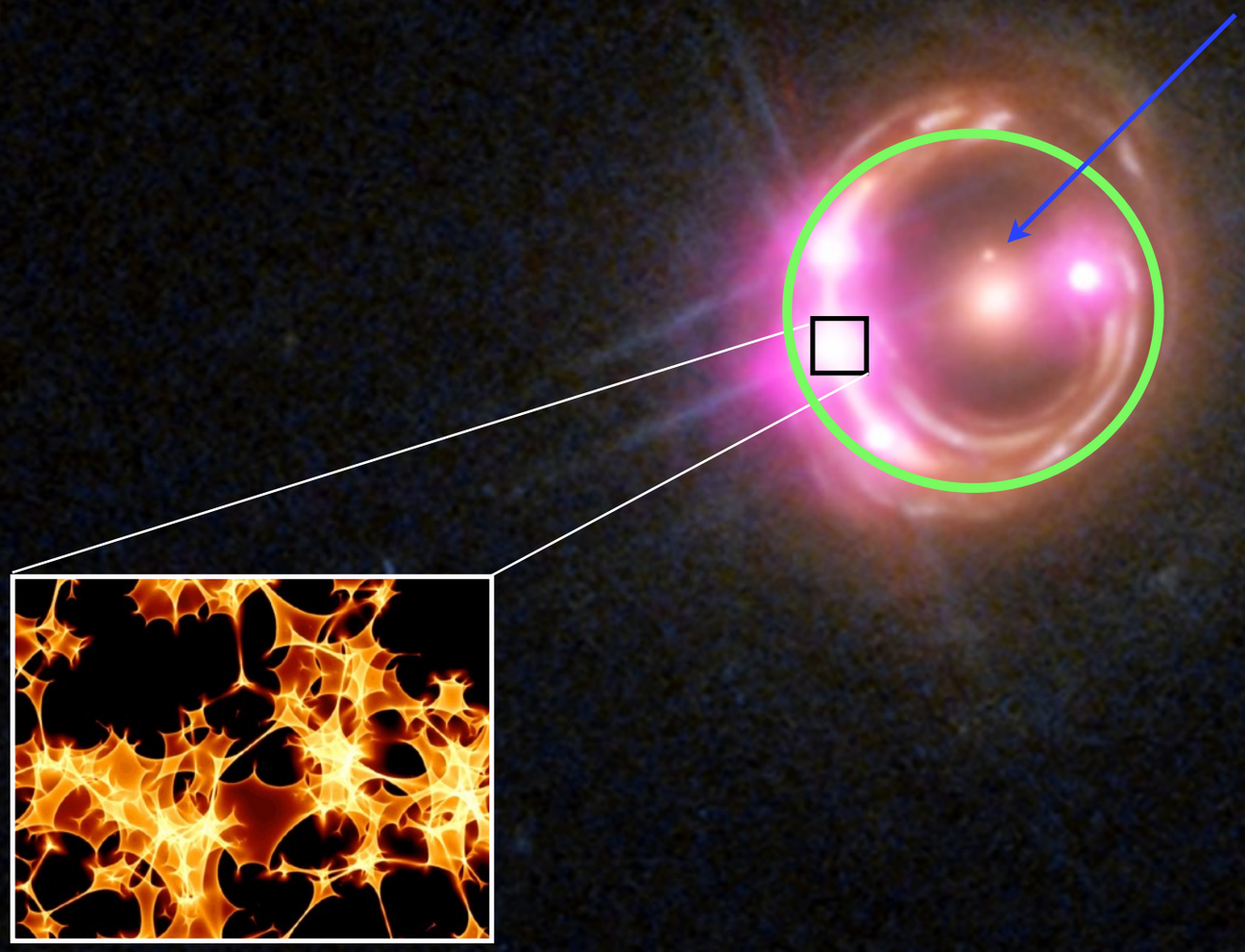

Microlensing

Image: NASA/STScI

# Basics of microlensing

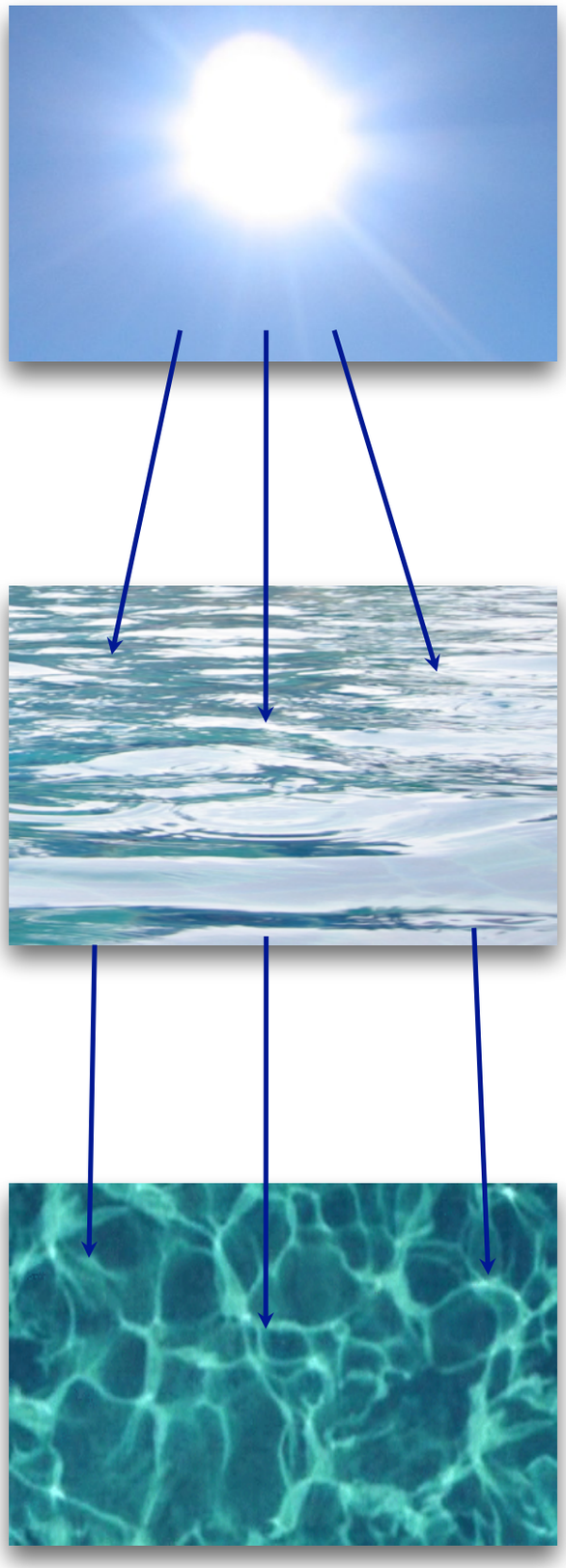

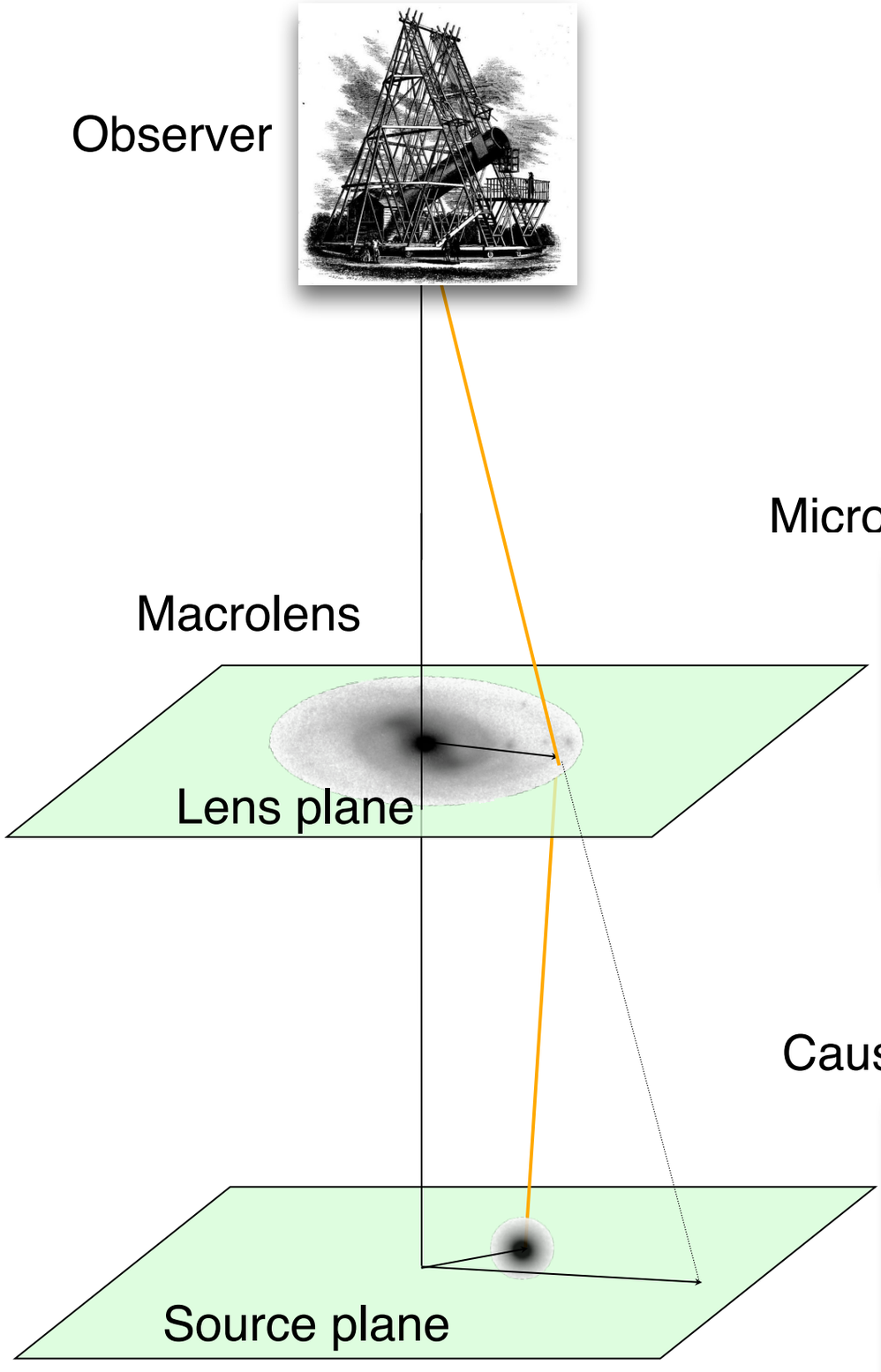


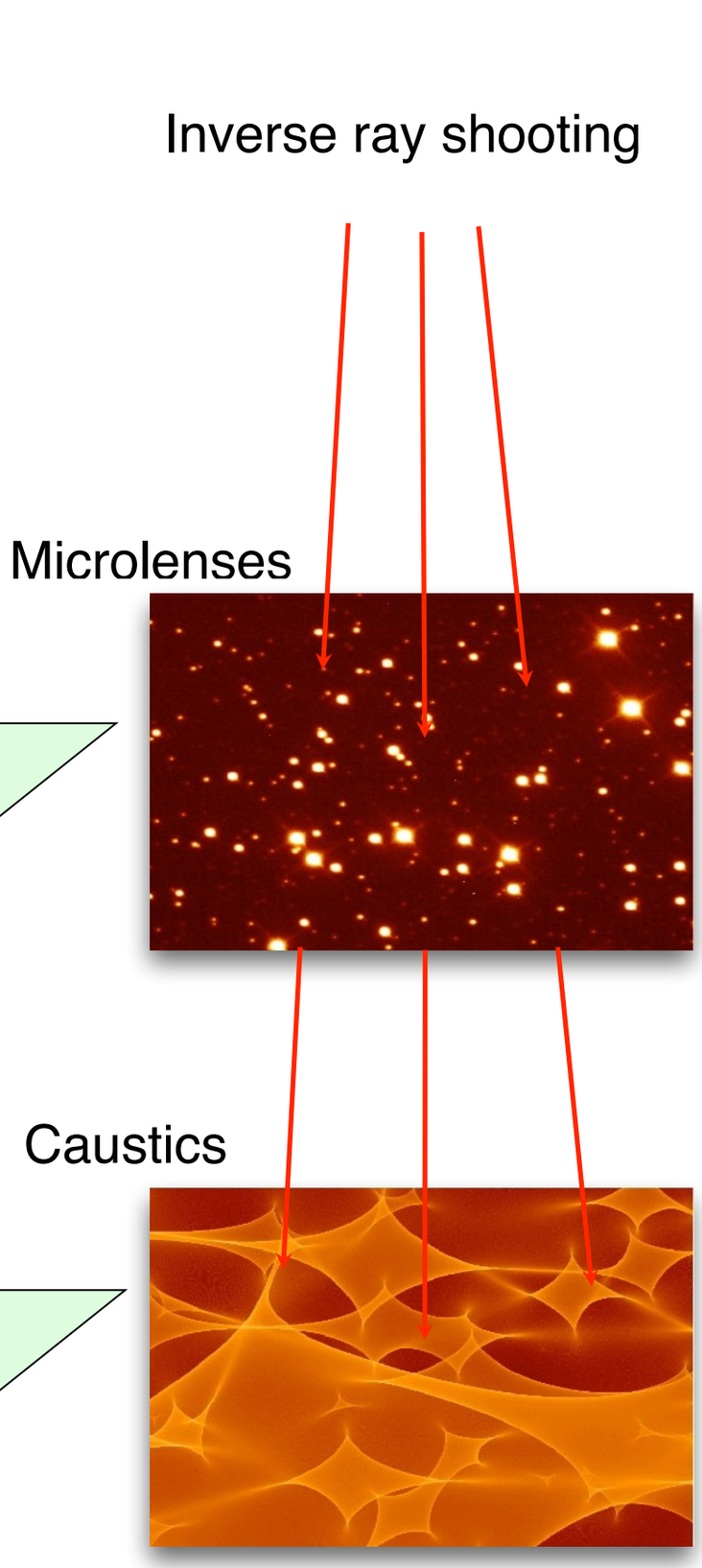

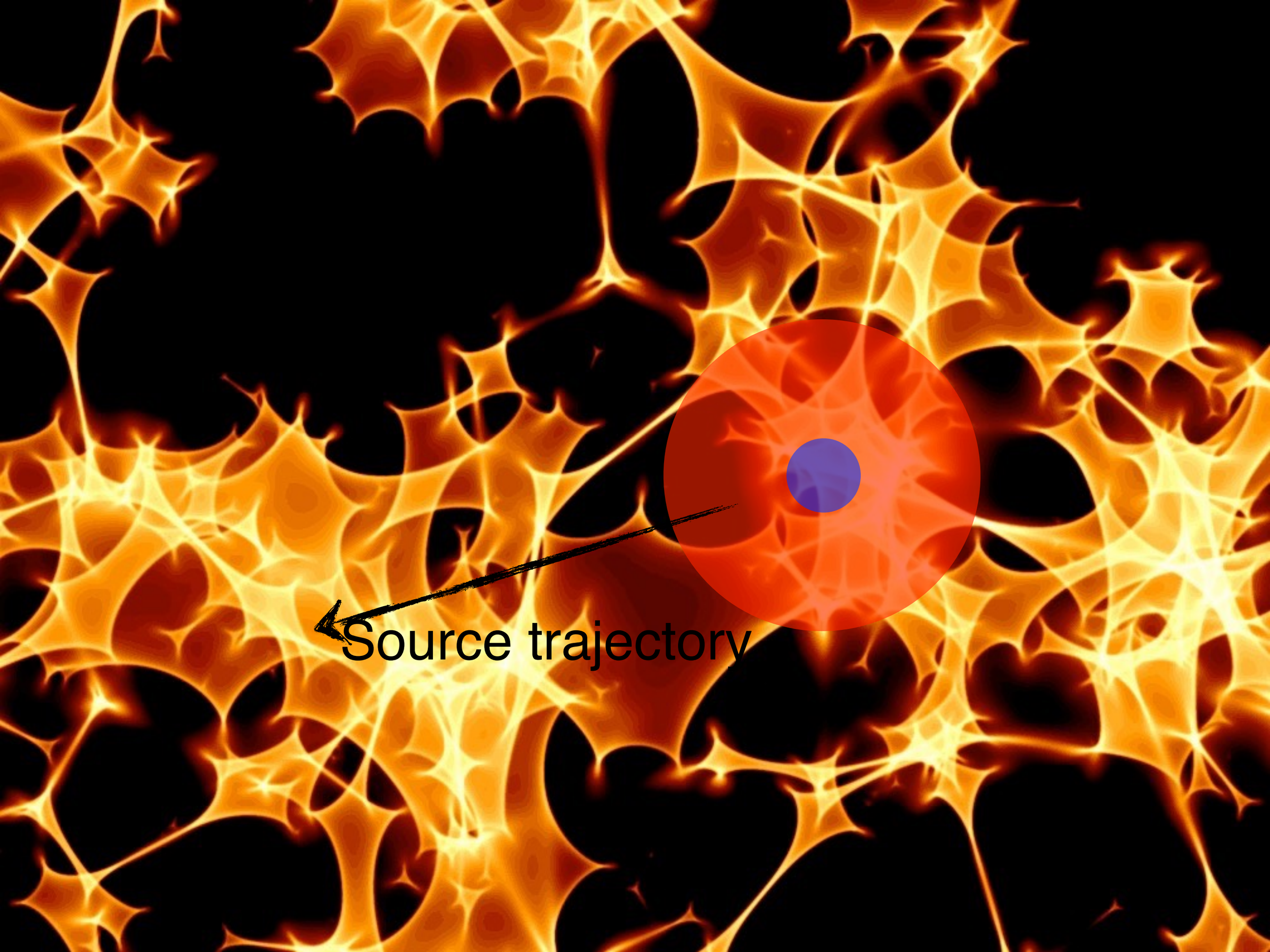
Source trajectory

# Example of strong microlensing

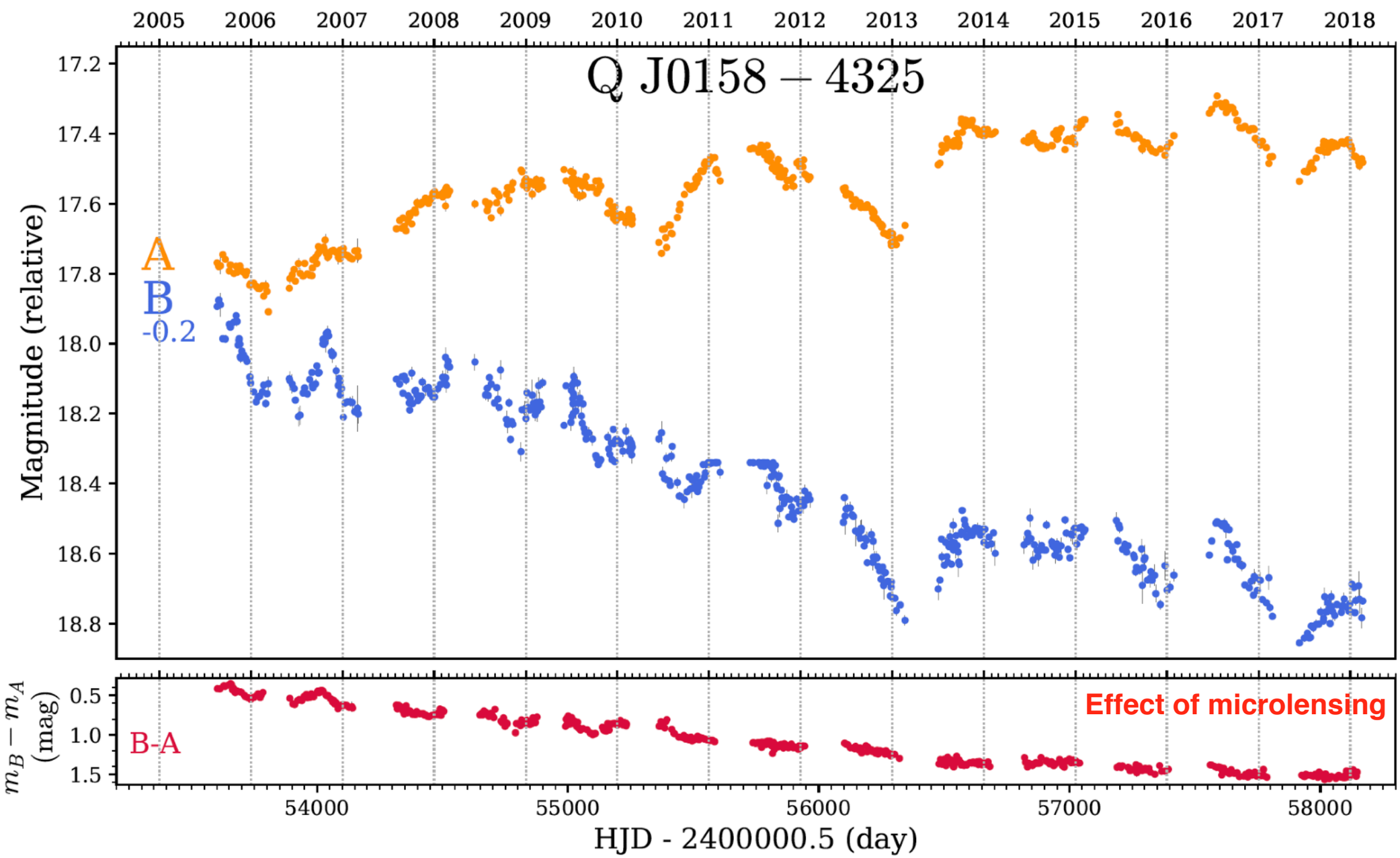


Source size using structures in the microlensing pattern
Energy profile of the source on parsec-scales
IMF of lensing galaxy
Measurement of fraction of smooth vs. compact dark matter in the lens

Millon et al. 2020
to be submitted
this week.

# Time Delays Measure the Hubble Constant $H_0$

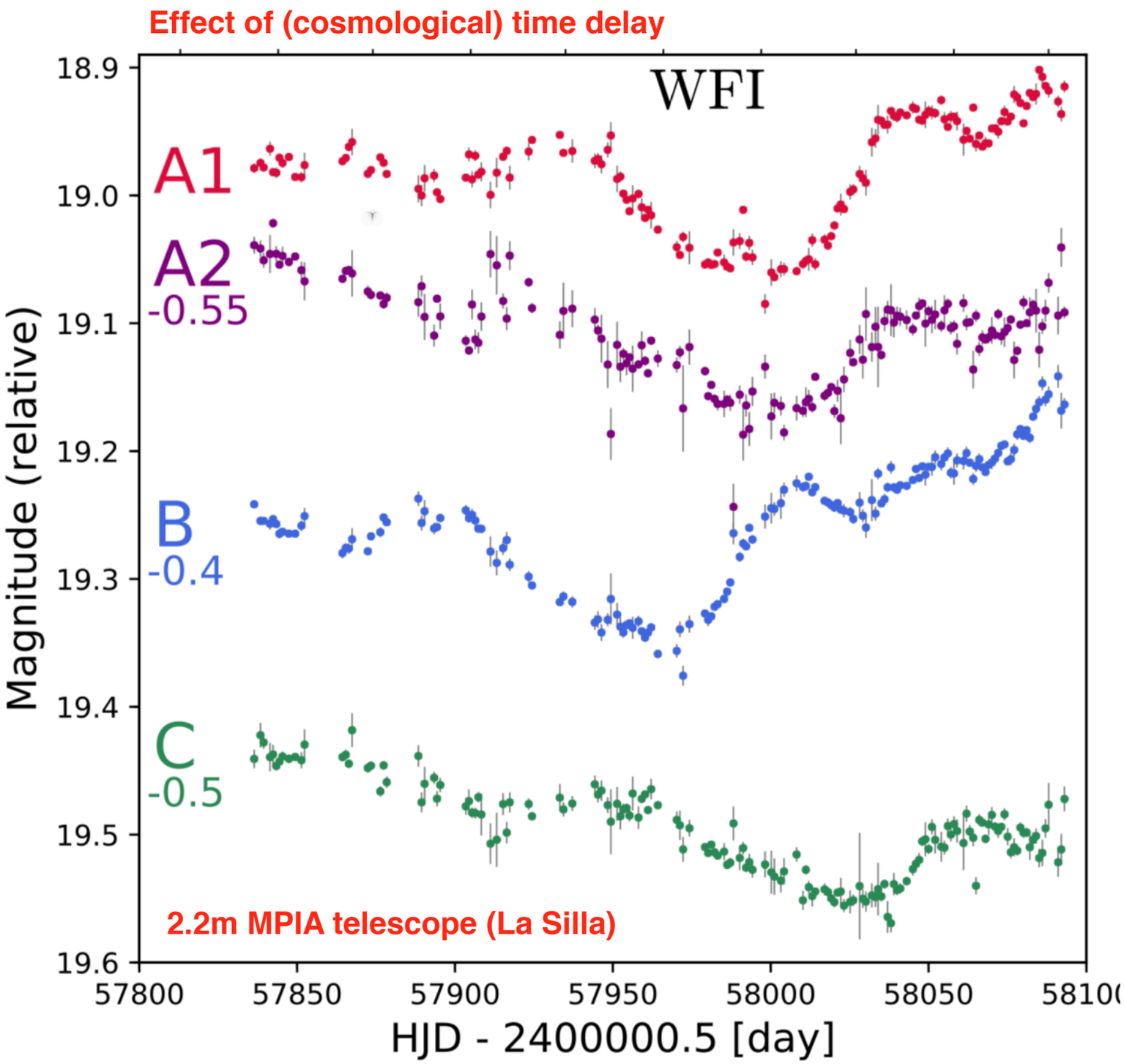


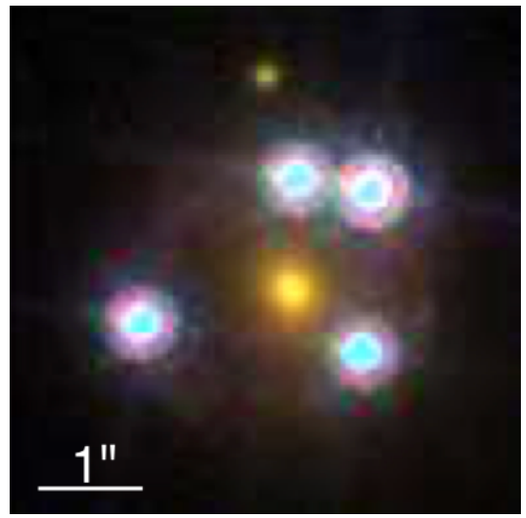


Bonvin et al. 2019

# Cosmology Results for 6 Lenses in flat lambda-CMD

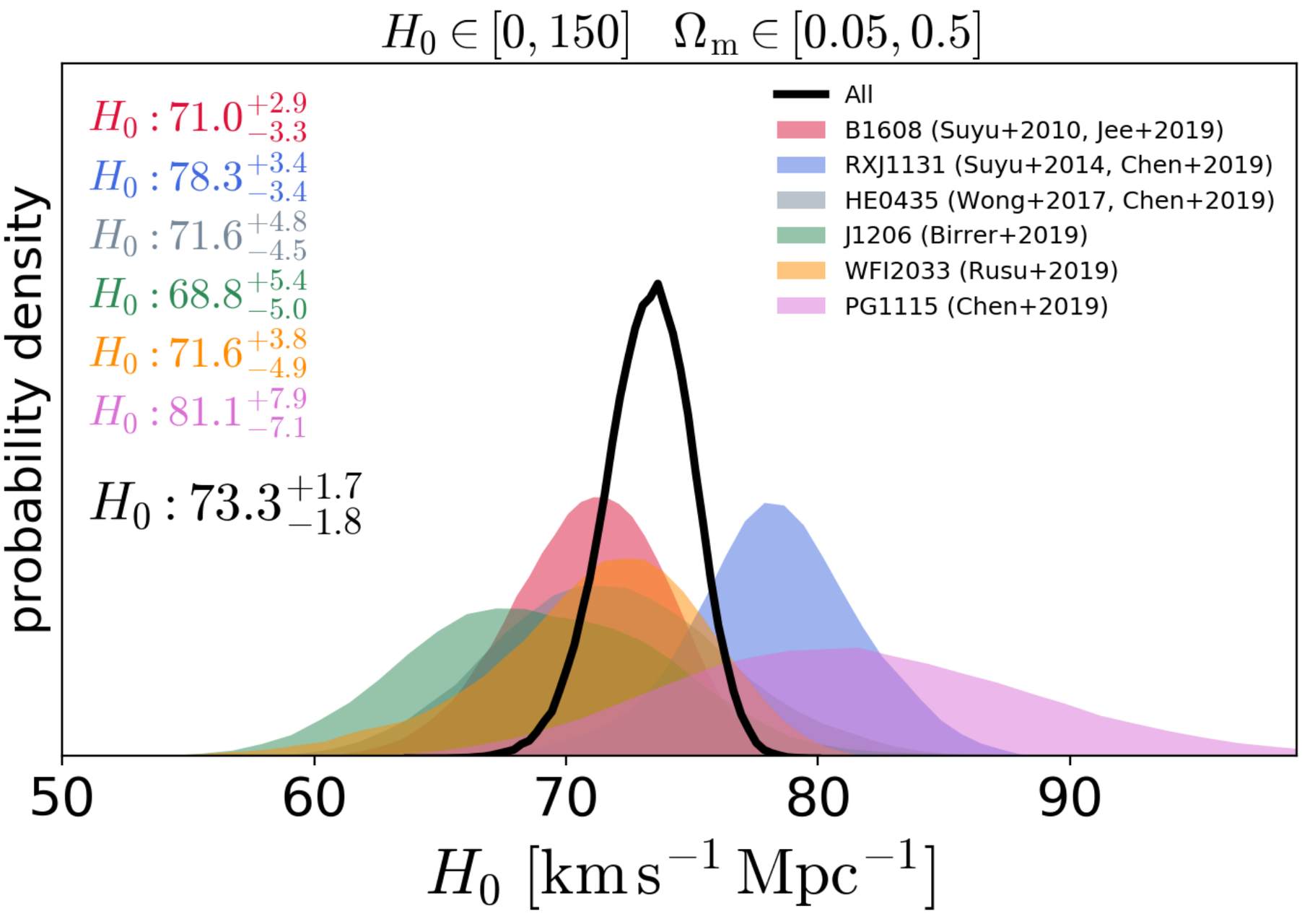


H0LiCOW XIII: milestone paper (Wong et al. 2019, arXiv1907.04869)

# Galaxy-scale strong lensing

- Mapping the radial mass slope of galaxies
- Stellar velocity dispersion in some spectroscopic aperture
- Total mass in the Einstein radius
- Comparing the total mass with the visible mass
- Allows to study the full radial mass profile when applying the technique to a sample of lenses with similar physical properties

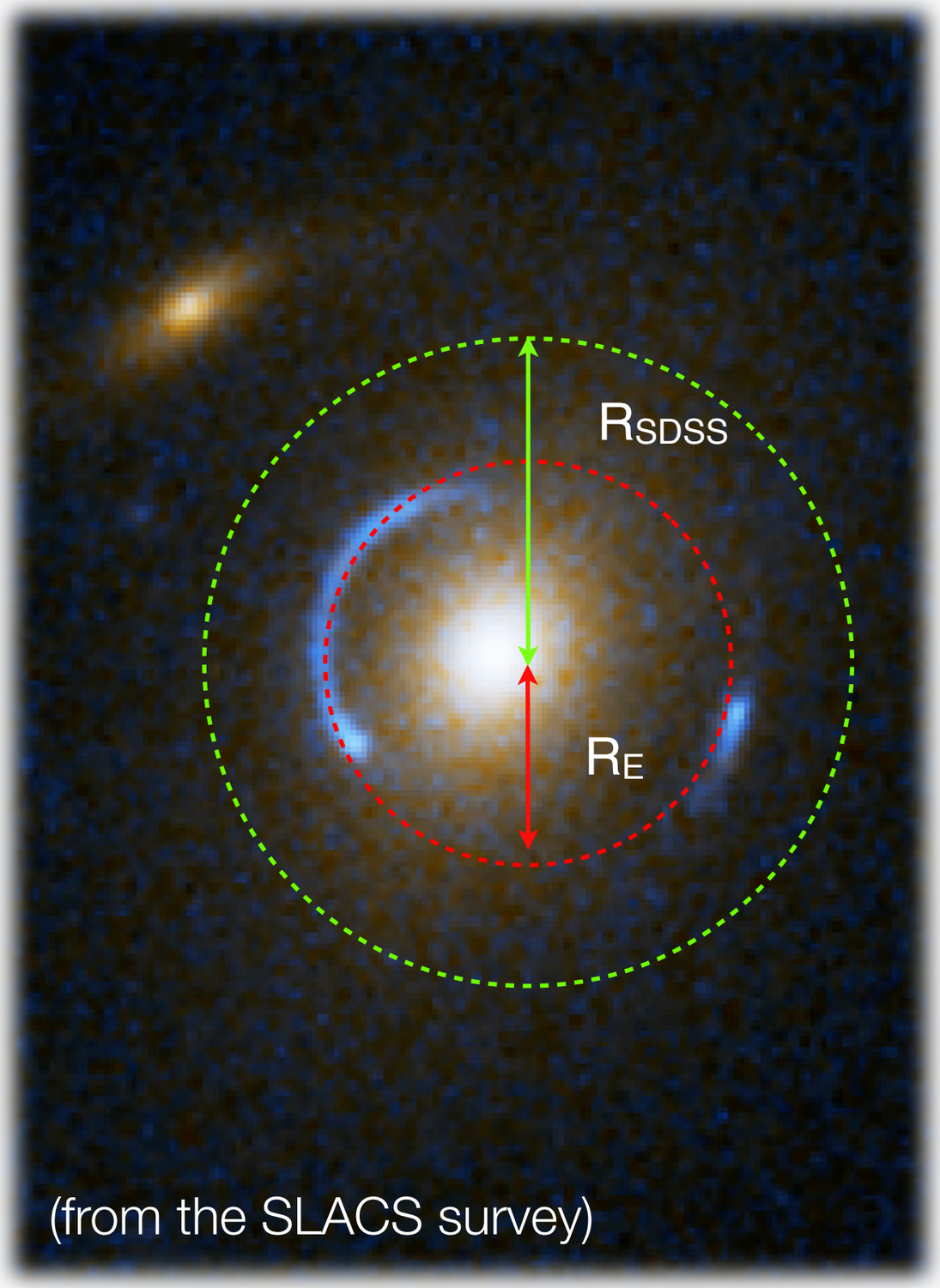

# Lensing BY quasars or AGNs

## Jackpot lenses #1

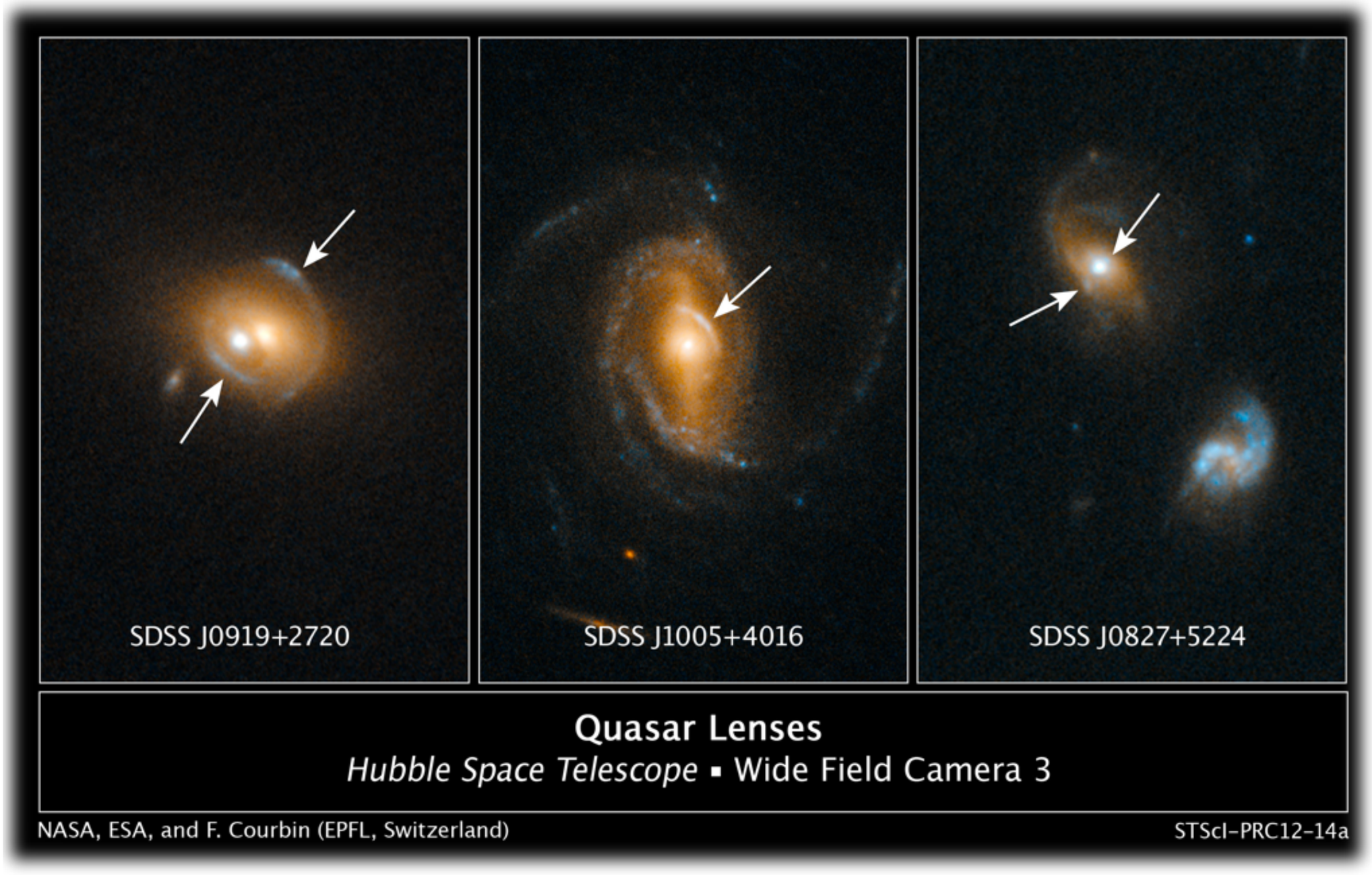


(Courbin et al. 2012, A&A 540, 36 - Millon et al. 2020, in prep)

# Distance Ratios from Sources at Multiple Redshifts

## Jackpot lenses #2

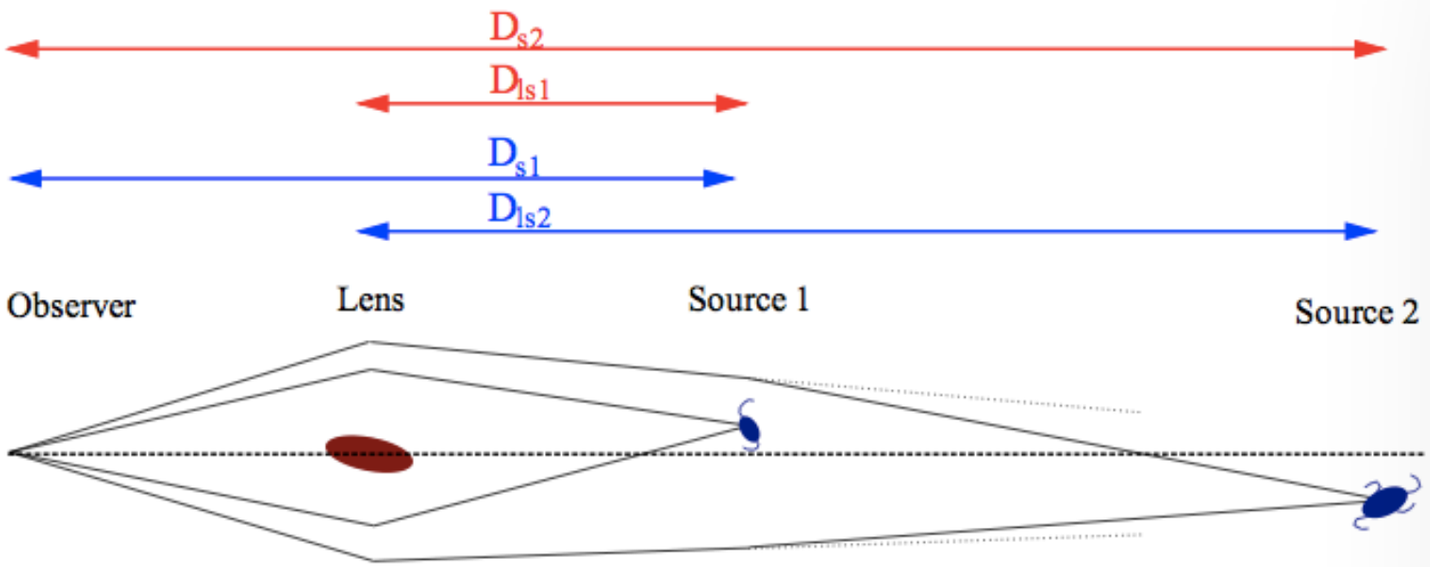


**Figure 1.** Sketch of a double source plane lens system. The cosmological scaling factor $\beta$ is the product of $D_{ls1}$ and $D_{s2}$ (both in red) divided by the product of $D_{ls2}$ and $D_{s1}$ (both in blue). For a singular isothermal sphere, where the first source has no mass, $\beta$ is the ratio of Einstein radii. Figure taken from Collett et al. (2012).

(Collett & Auger, 2014, MNRAS 443, 969)
(Collet et al. 2012, MNRAS 424, 2864)

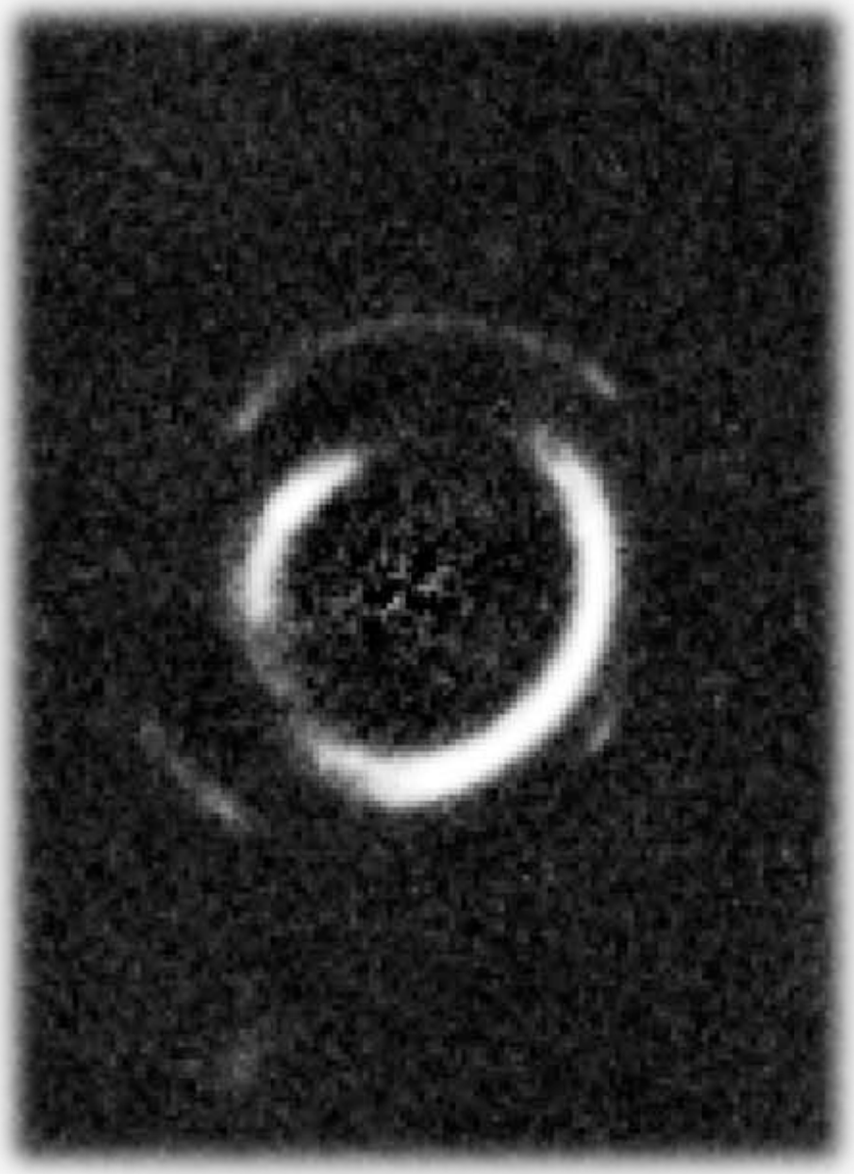

(Gavazzi et al. 2008, ApJ, 677, 1046)

# Distance Ratios from Sources at Multiple Redshifts

- **Tomography** using sources at different redshifts
- Measure $\mathbf{D_{ls}/D_s}$ **ratios** for sources at different redshifts
- Done so far in Abell 1689 using 28 multiple images

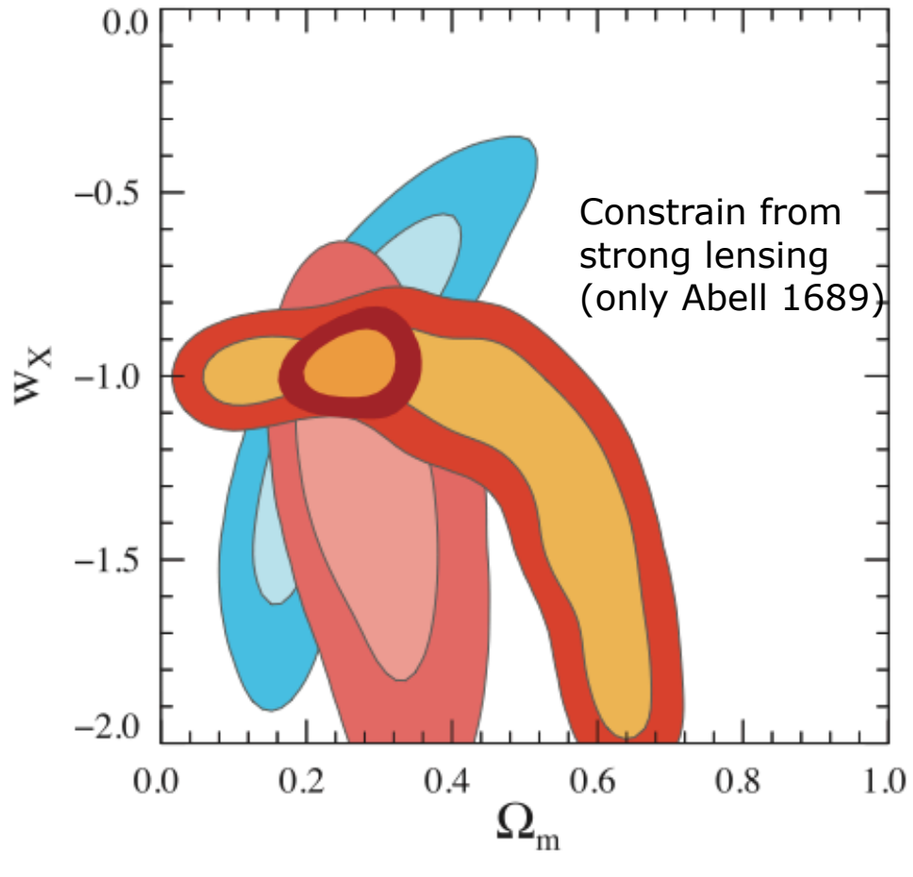


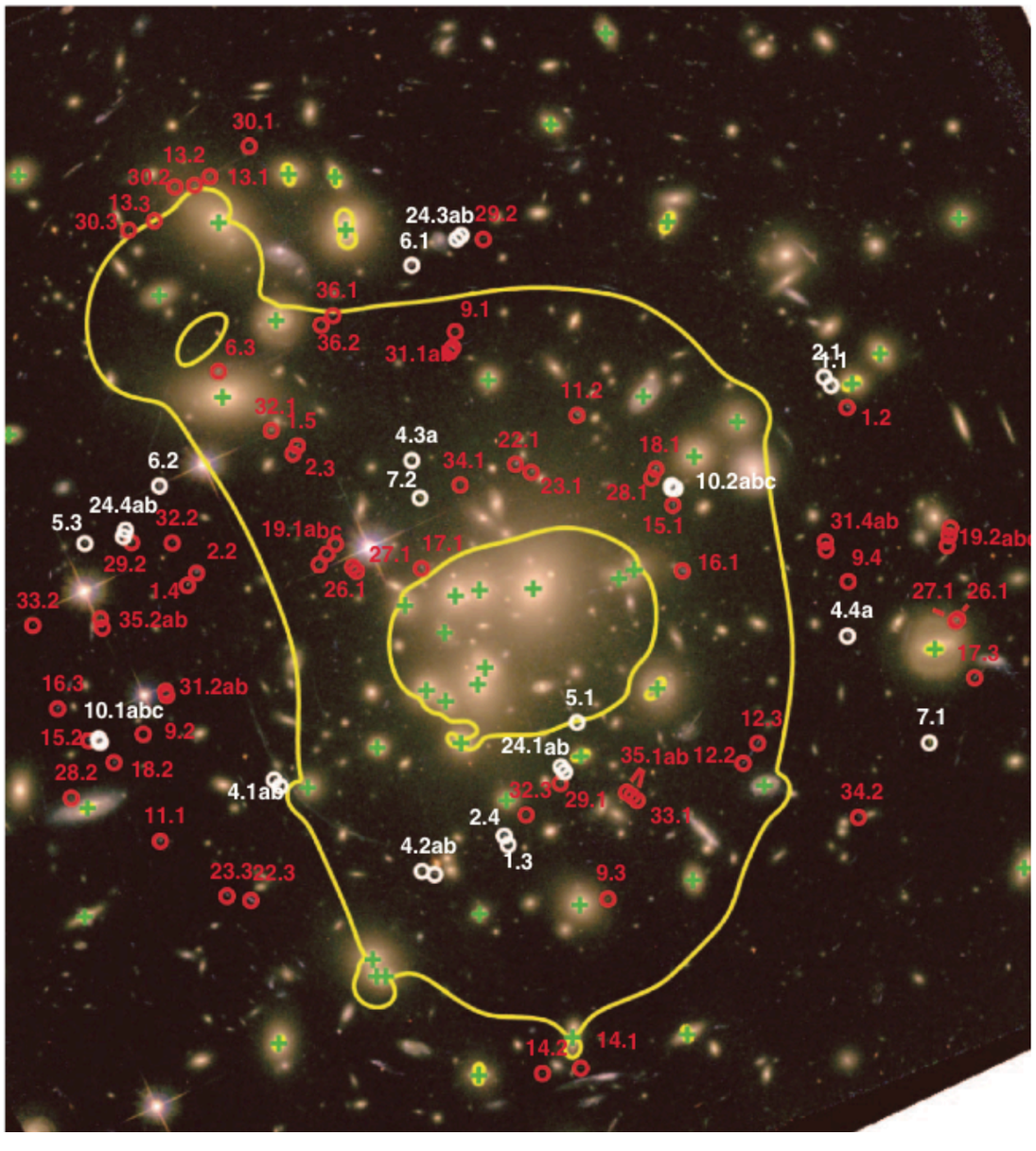


(Jullo et al. 2010, Science, 329, 924)

# Flux ratio anomalies and substructures

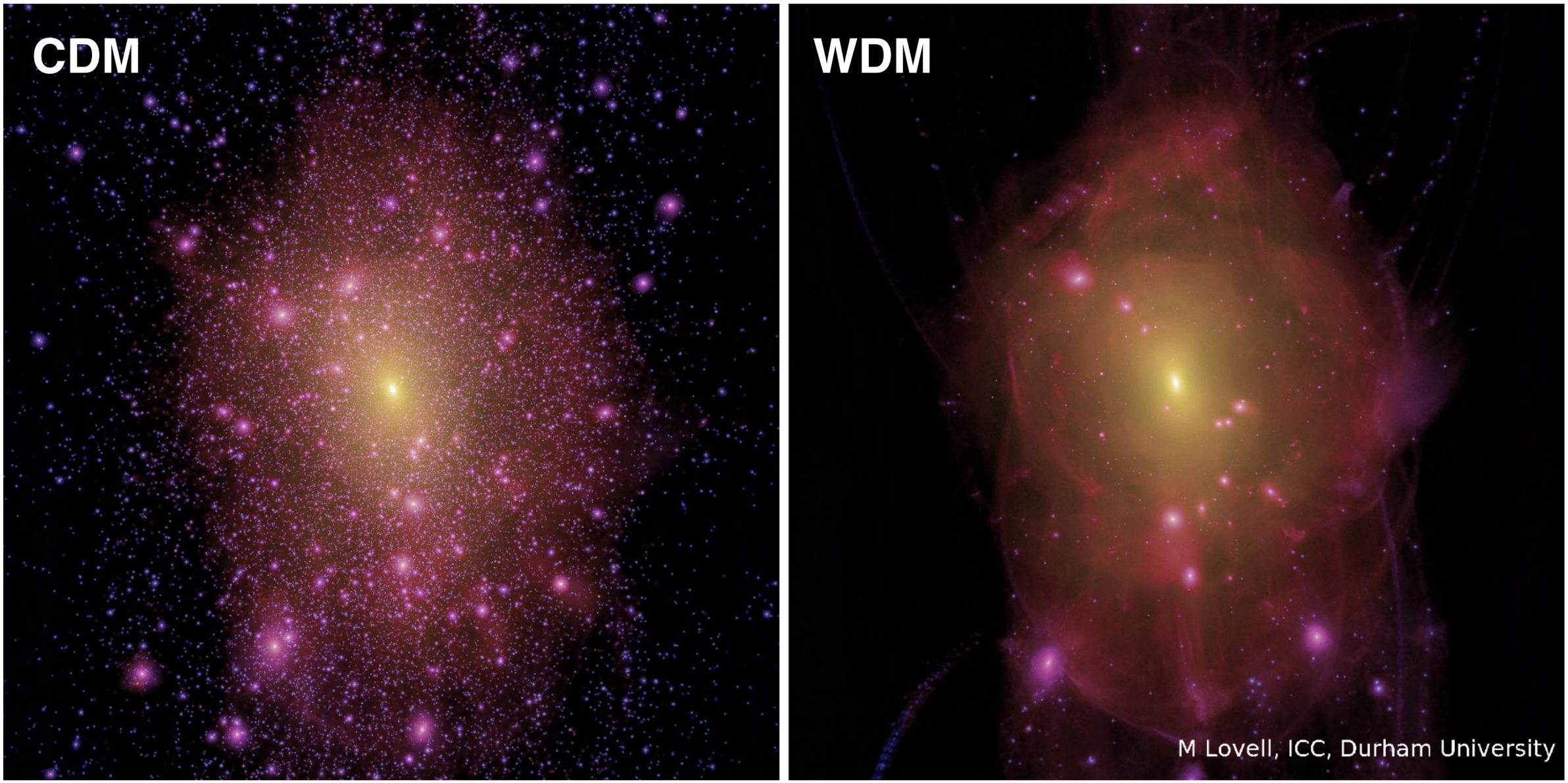


**CDM forms more substructures than WDM and this is observable with lensing (but beware of the effect of baryons…)**

# Flux ratio anomalies and substructures

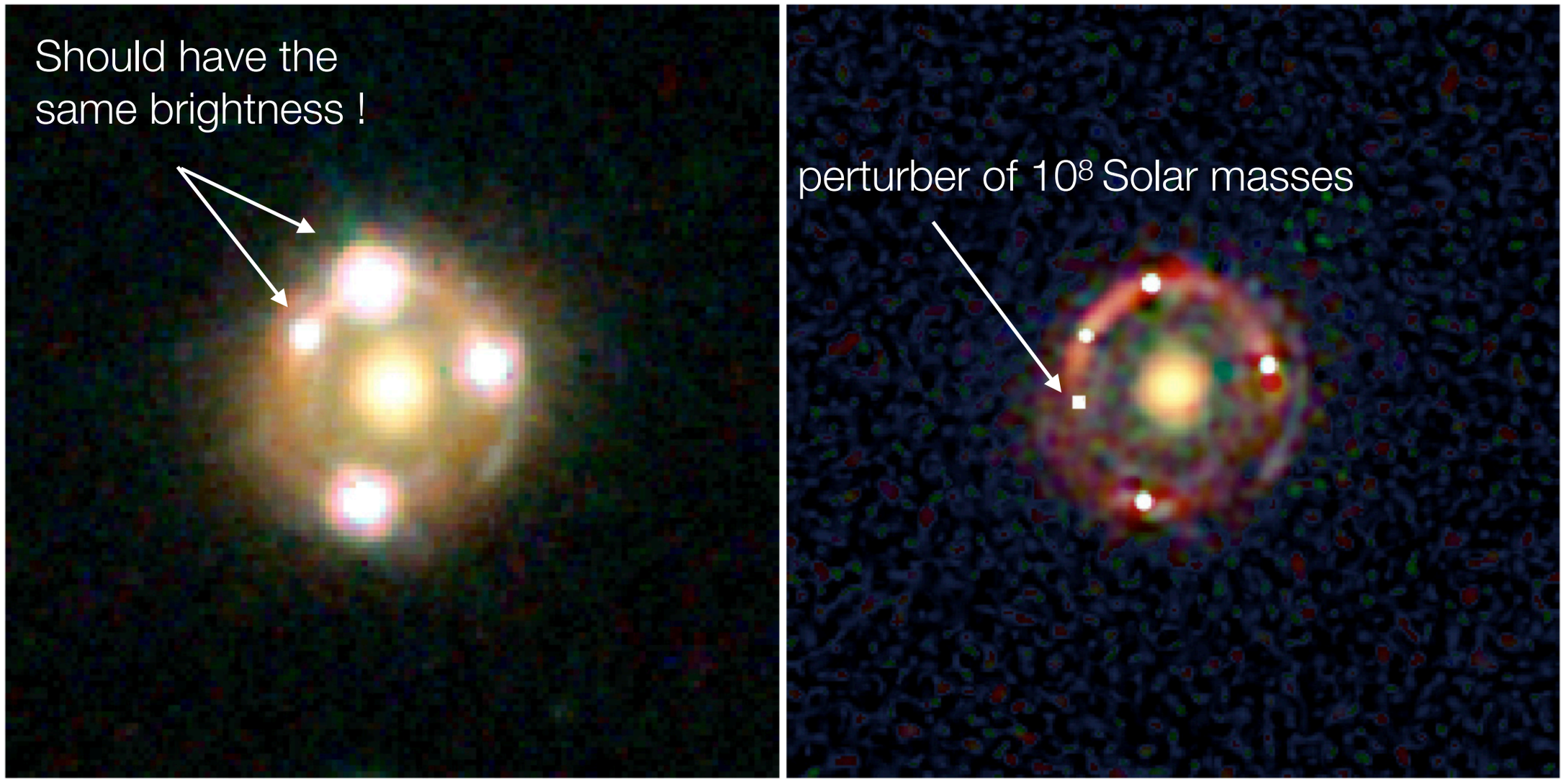


**Fig. 11.** *Left*: composite HST image using the observations through the *F555W*, *F814W* and *F160W* filters. The resolution is respectively 0.10″ in *F555W* and *F814W*, and 0.15″ in *F160W*. *Right*: deconvolved image. It has a pixel size of 0.025″ and a resolution of 0.05″. The lensed host galaxy of the quasar is clearly seen as red arcs well centered on the quasar images. A second set of bluer arcs inside and outside the area delimited by the red arcs is also revealed. The field of view is 3.0″ on a side. The image is slightly rotated relative to North, which is at PA = –2.67°. East is to the left. The white square shows the position of the perturber found for the SIE and NFW models of Sect. 5.2.

Eigenbrod et al. 2006, A&A 451, 747
More recent: Gilman et al. 2020, MNRAS 491, 6077
Nierenberg et al. 2020, MNRAS in press

# Samples of lensed quasars

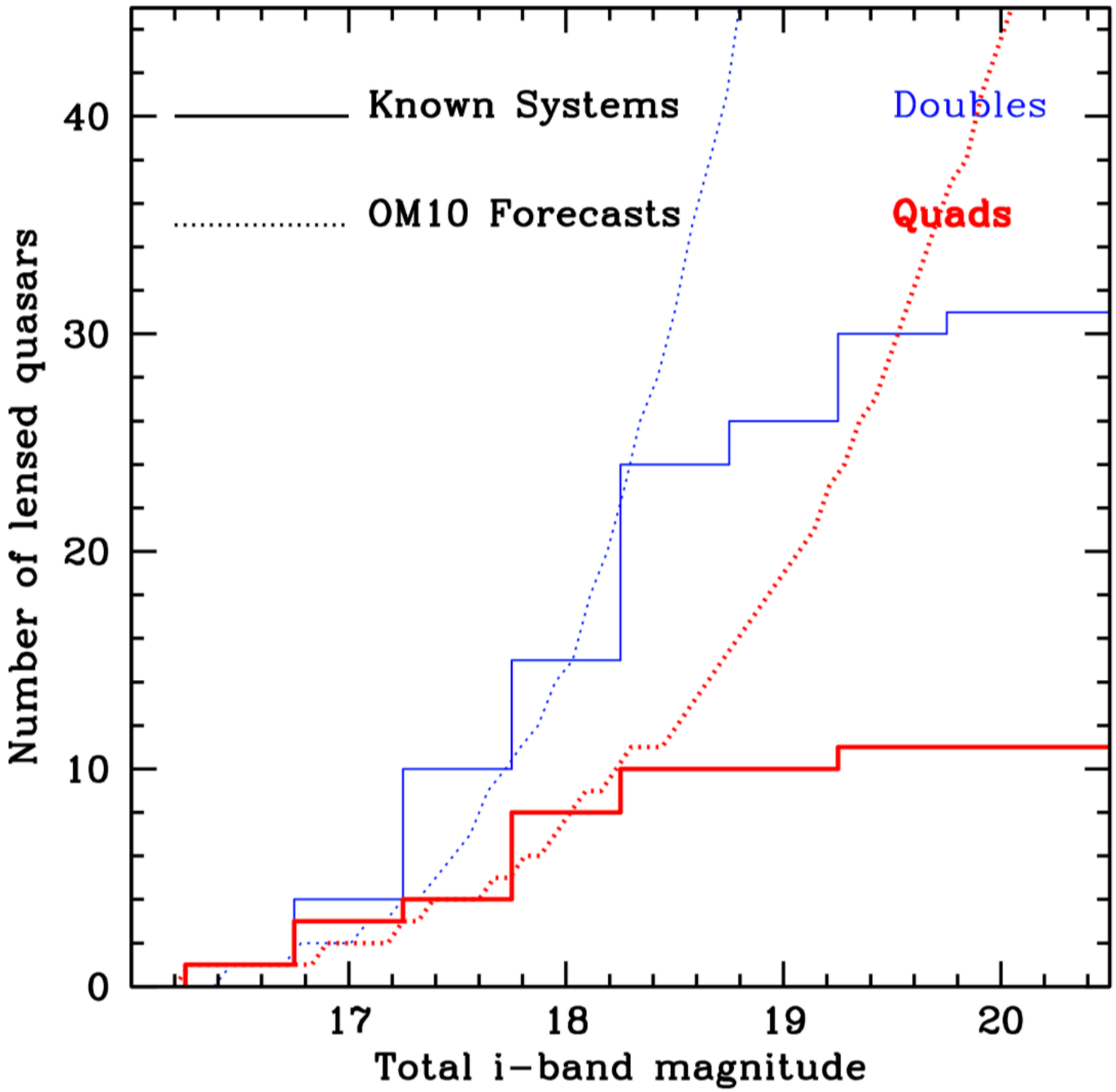


Treu et al. 2018, MNRAS 481, 1041
+ recent papers by Lemon et al.
Most efficient searches use variability + Gaia + color information

# Samples of flux ratios (in doubles)

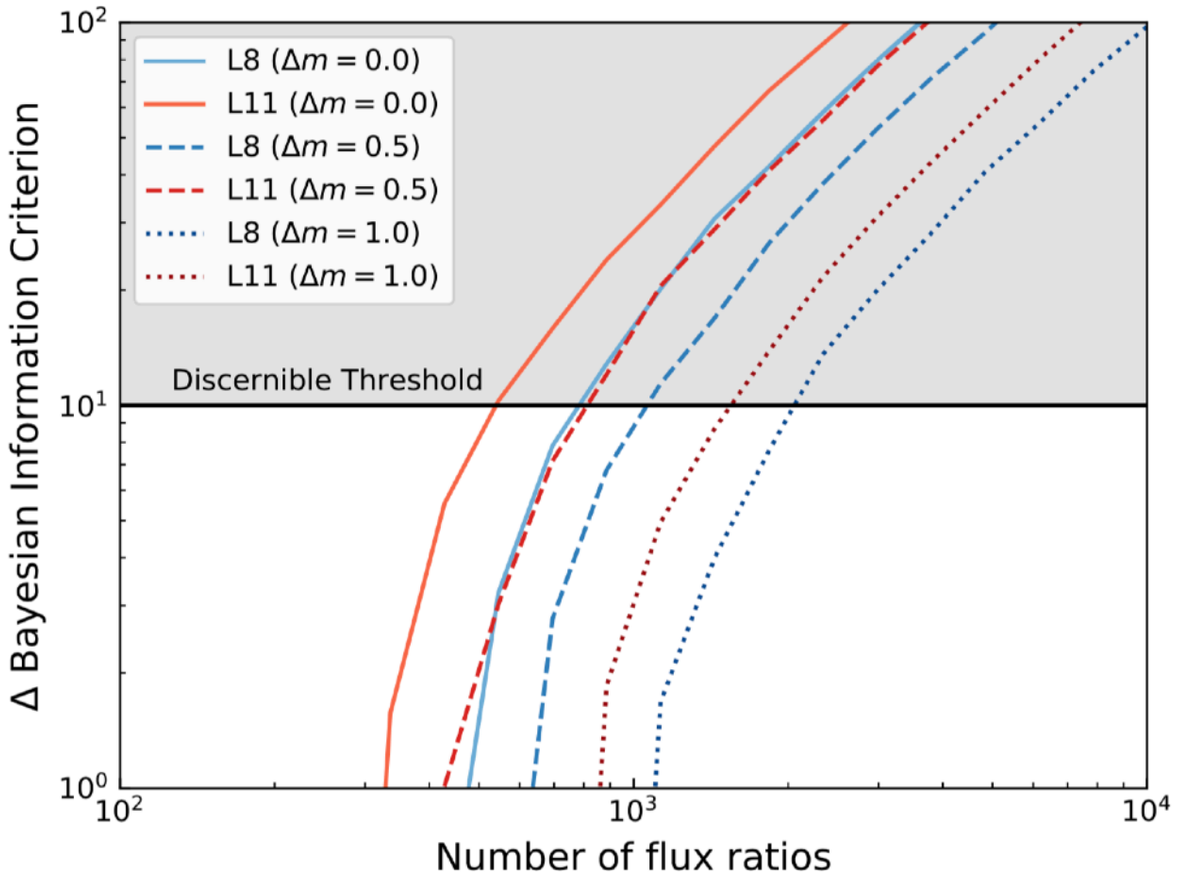


**Figure 3.** The change in Bayesian information criterion, an estimator for choosing between two models, for the two WDM models considered in this study. A $\Delta$BIC $> 10$ is considered very strong preference for one model over another and the threshold to rule out a particular model of dark matter. Here, we show the required number of flux ratios to be able to unambiguously discern between either the CDM model or the paired WDM model, (L8 in blue and L11 in red) for three values of quasar variability; $\Delta m = 0$ (solid line), $\Delta m = 0$ (dashed line), and $\Delta m = 1.0$ (dotted line).

$$L_6 = (n_{\nu_e} - \bar{n}_{\nu_e})/s$$

$L_6$ = 8 coldest WDM 7 keV neutrino

$L_6$ = 11.2 warmest consistent with resonantly-produced sterile neutrino decay interpretation of the 3.55 keV line

**A few hundreds of doubly-images are needed and can be found with Euclid**

Harvey et al. 2020, MNRAS 491, 4247

# Probing Substructures Using Lensed Arcs

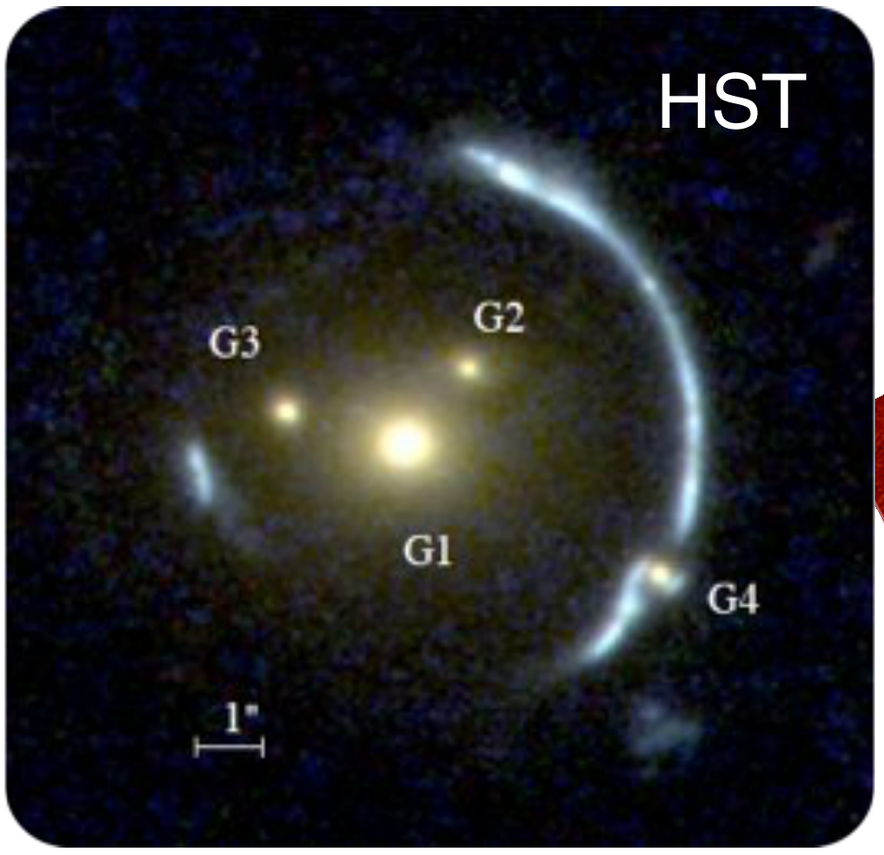


The “Clone” system
Lin et al. 2009

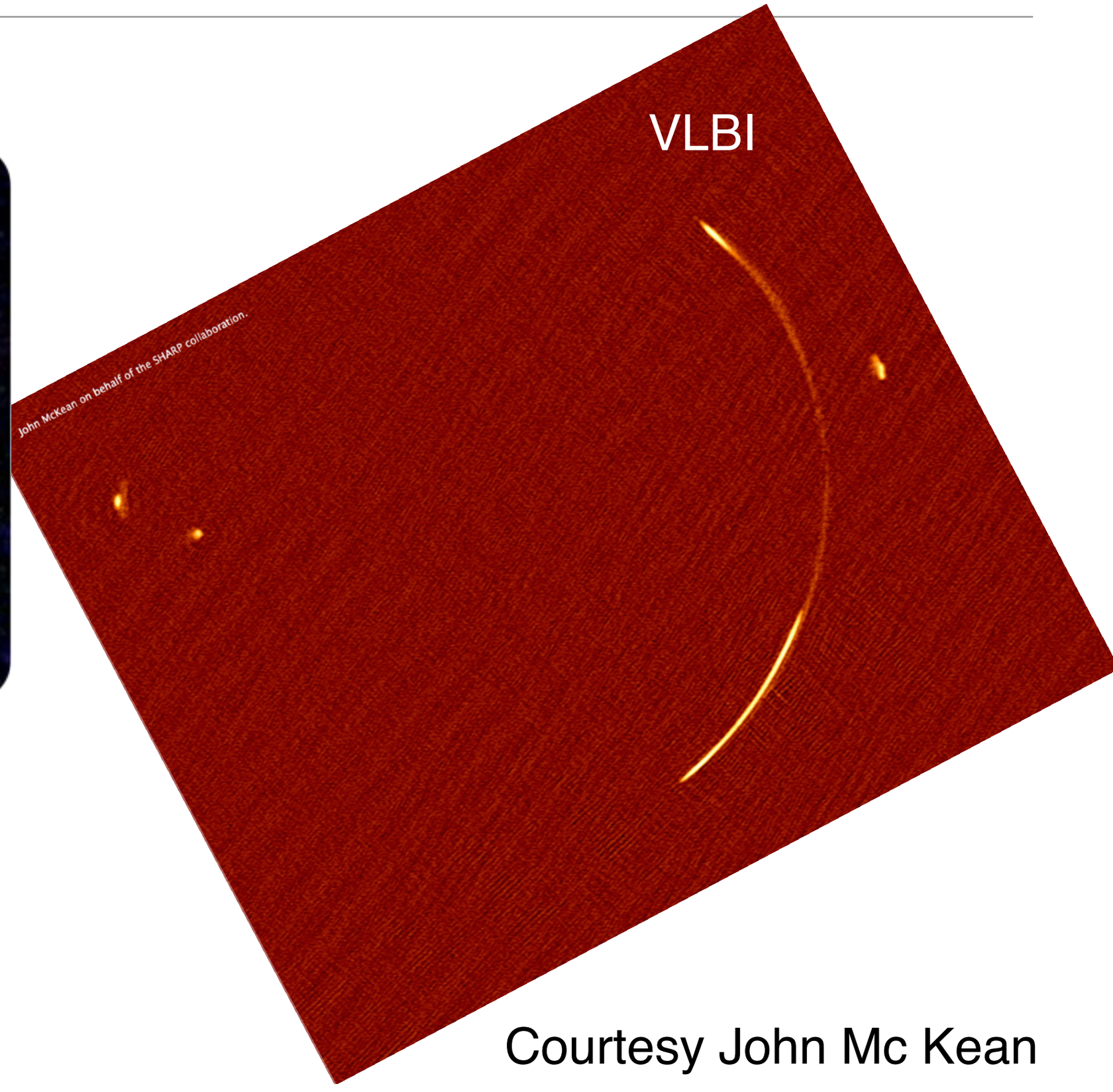


Courtesy John Mc Kean

# Probing Substructures Using Lensed Arcs

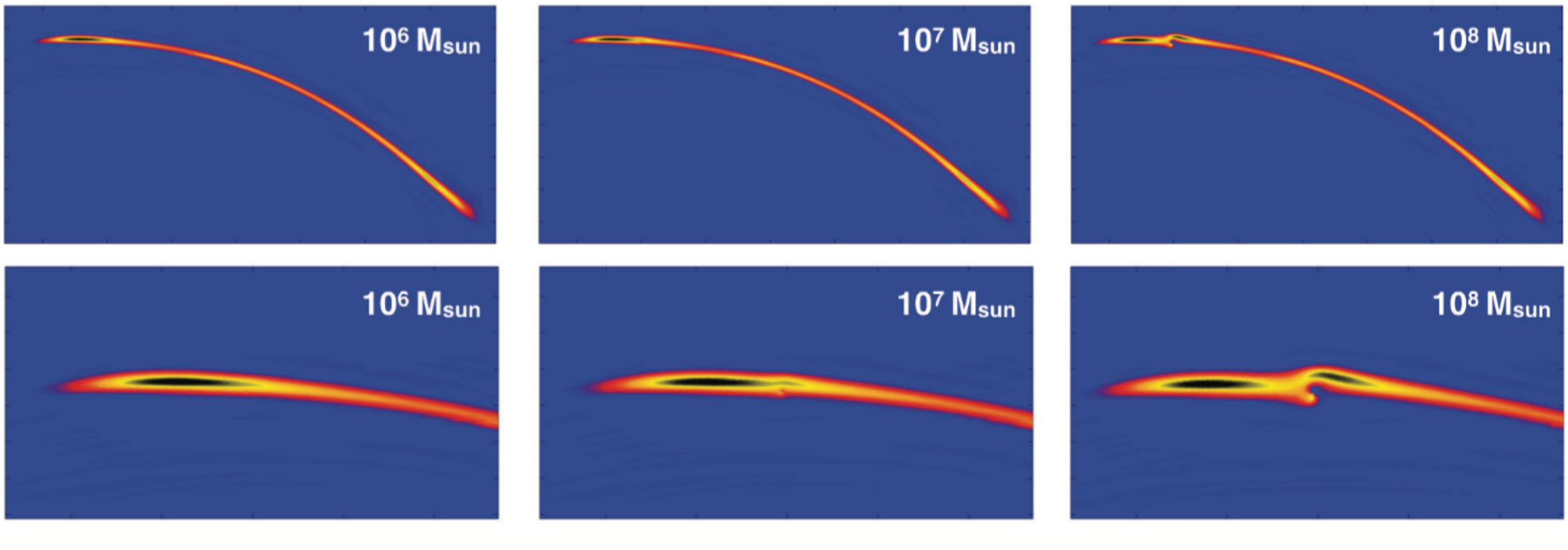


**Figure 5:** Simulations of the effect low mass dark matter haloes have on arc surface brightness distributions for a $10^6$ $M_\odot$ (left), $10^7$ $M_\odot$ (middle) and $10^8$ $M_\odot$ (right) substructure. The top row of images show the full gravitational arc, detected on VLBI scales with an SKA1-MID+VLBI array, and the bottom row show a zoomed in view of the region most affected by the substructure. The $10^7$ $M_\odot$ and $10^8$ $M_\odot$ substructures can be seen directly in the data, whereas the $10^6$ $M_\odot$ substructure would need to be detected using the gravitational imaging technique.

Gravitational lensing “imaging” is sensitive to $10^7$ Solar masses !

From Mc Kean et al. SKA science book (but this works for Euclid as well !)

# Strong lensing with Euclid in numbers

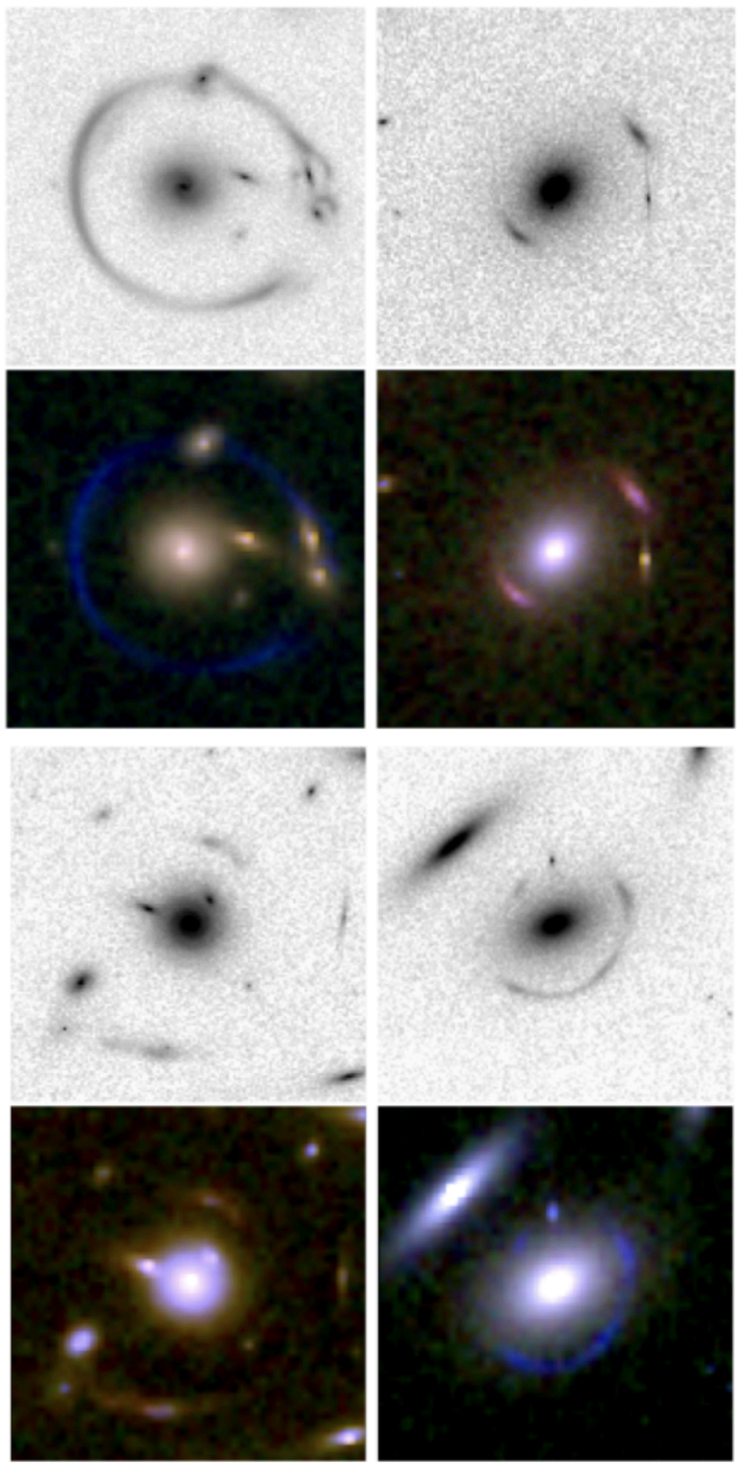

Examples of Euclid galaxy-scale lenses
From Euclid SL-SWG white paper, 2020, to be finished !

Cluster lenses: ~ 10’000 (giant arcs)

Galaxy lenses: ~ 200’000 (early type only)
+500 in the deep fields

Jackpot lenses: ~ 100 (double source plane)

Lensed quasars: ~ 5’000

Quasar lensing: ~ 100 (quasars lensing galaxies)

Lensed H alpha: ~ 3’000 (Euclid spectra)

Lensed SNIa (in combination
with LSST): ~ 20

WILL NEED FOLLOW UP FACILITIES !

# Organization of strong lensing work

- Lens finding algorithms are part of OU-SHE (lead: Courbin)
- Strong lensing Science Working Group (SL-SWG - leads: Gavazzi, Kneib, Meneghetti)
- Meeting of the group twice per year
- Pre-Launch Key Projects on clusters and galaxies defined in Paris in October 2019
- Lens-finding algorithms at Swiss SDC at Ecogia + France
- Talk by Elodie Savary (lensing finding challenge)
- Talk by Karina Rojas (lens finding with Machine Learning)
- Talk by Benjamin Clément (lens finding pipeline)

**PLEASE feel free to join the SL-SWG and lens finding efforts**